Tikrit Journal of Engineering Sciences (2024); 31(4): 34-45
DOI: http://doi.org/10.25130/tjes.31.4.4

IRAQI Academic Scientific Journals

ISSN: 1813-162X (Print); 2312-7589 (Online)
Tikrit Journal of Engineering Sciences
available online at: http://www.tj-es.com

TJES Tikrit Journal of Engineering Sciences

Flow Characteristics in Vertical Shaft Spillway with Varied Inlet Shapes and Submergence States

***Intisar A. Hady*, *Ahmed Y. Mohammed* ***
Dams and Water Resources Engineering College of Engineering, University of Mosul, Mosul, Iraq.

Keywords:
Shaft spillway; Flow regime; Spillway; Tail water; Flow conditions; Discharge coefficient.

Highlights:

- *Four physical models of vertical shaft spillways with different edge shapes were used to study the flow characteristics.*
- *Three free, semi, and submerged tailwater heights were studied to find their effects on the discharge coefficient.*
- *Two flow cases at the shaft spillway entrance were observed, depending on the water depth upstream: weir flow and orifice flow.*
- *An increase in the length of the entrance edge shape resulted in a high spillway discharge and a low upstream water depth.*

ARTICLE INFO
Article history:

Received	09 June	2023
Received in revised form	02 Sep.	2023
Accepted	08 Jan.	2024
Final Proofreading	27 May	2024
Available online	24 Nov.	2024

Citation: Hady IA, Mohammed AY. **Flow Characteristics in Vertical Shaft Spillway with Varied Inlet Shapes and Submergence States.** *Tikrit Journal of Engineering Sciences* 2024; **31**(4): 34-45.
http://doi.org/10.25130/tjes.31.4.4

***Corresponding author:*

Ahmed Y. Mohammed
Dams and Water Resources Engineering College of Engineering, University of Mosul, Mosul, Iraq.

Abstract: A spillway is an essential hydraulic structure that discharges excessive water, especially during floods from upstream to downstream of the dam. A shaft spillway is sometimes used when a limited area is available. This study used four physical models of vertical shaft spillways with different edge shapes to study the flow characteristics. Each case was based on three tailwater heights: free, semi, and submerged. The results showed that two flow cases at the entrance depended on the water depth upstream; the weir flow happened at low discharge when the ratio of water depth to shaft diameter H/D was less than 0.5, and orifice flow when the proportion H/D was greater than 0.5. In the weir flow regime for submerged conditions, the water depth upstream (H) decreased by (6%) more than free flow. When replacing inlet shapes, the upstream depth (H) decreased by (40%) in the weir flow and (13%) in the orifice flow. In weir flow, the discharge coefficient values decreased with crest length, and larger values were obtained at the submerged state. While in orifice flow, Cd values increased with crest length, and higher values occurred at semi-submerged. Spillway discharge increased with entrance edge shape length in submerged condition.

خصائص الجريان في المطفح العمودي باشكال مدخل وحالات غمر مختلفة

انتصار أزهر هادي، احمد يونس محمد
قسم هندسة السدود والموارد المائية / كلية الهندسة / جامعة الموصل /الموصل – العراق.

الخلاصة
المطفح المائي هو منشأ هيدروليكي يقوم بتصريف المياه الزائدة، خاصة أثناء الفيضانات من أعلى مجرى السد إلى أسفله. يتم استخدام مجرى التدفق في بعض الأحيان عند توفر مساحة محدودة. في هذه الدراسة، تم دراسة أربعة نماذج فيزيائية للمطفح العمودي بأشكال حواف مختلفة لدراسة خصائص الجريان للمطفح العمودي. كل حالة تعتمد على ثلاثة ارتفاعات للماء الذيلي: (حر، شبه مغمور ومغمور بالكامل). أظهرت النتائج وجود حالتين للجريان عند مدخل المطفح اعتمادًا على عمق الماء في المقدمة؛ جريان السد الغاطس عند التصاريف المنخفضة عندما تكون نسبة عمق الماء إلى قطر العمود H / D أقل من ٠,٥. وجريان الفتحة الحادة عندما تكون نسبة H / D أكبر من ٠,٥. في نظام جريان السد الغاطس للحالة المغمورة، ينخفض عمق الماء عند المنبع (H) بنسبة (٦٪) مقارنة بالجريان الحر. عند استبدال أشكال المدخل، ينخفض العمق (H) بنسبة (٤٠٪) في جريان السد الغاطس، و (١٣٪) في جريان الفتحة الحادة. في جريان السد الغاطس، تنخفض قيم معامل التصريف عندما يزيد طول الحافة، وترتفع القيم عند الحالة المغمورة. أثناء جريان الفتحة الحادة، تزداد قيم Cd عندما يزداد طول الحافة وتحدث القيم الأعلى عند الحالة شبه المغمورة. يزداد تصريف المطفح عندما يزيد طول حافة المدخل وفي الحالة المغمورة.

الكلمات الدالة: المطفح العمودي، حالة الجريان، المطفح، الماء الذيلي، حالات الجريان، معامل التصريف.

1.INTRODUCTION

A vertical shaft spillway is one of the structures used to discharge profuse water from a dam reservoir. Also, it can measure the discharge and, as a vertical intake, change the stream river in mountainous areas when creating a dam. This type of spillway is usually constructed in narrow valleys where it is hard to build a different kind of spillway in an earth or rock dam where the spillway must be built far away from the dam body and inside the dam reservoir to reduce the risk of overtopping [1, 2]. The effect of polyhedral spillway crests on the discharge intensity of the flow passing through the spillways and the discharge coefficient of Morning Glory spillways using a polyhedral spillway inlet was investigated. The polyhedral spillway inlet increased discharge passing through the Morning Glory Spillway and the spillway's discharge coefficient [3]. The effect of the angle, number, and thickness of the anti-vortex plates on the discharge coefficient of the shaft spillway was explored. The results showed that reducing the angular alignment of the anti-vortex plates on a spillway increased the coefficient of discharge rate, and five anti-vortex plates created the maximum discharge coefficient with an angle of 60 degrees [4]. The effect of different slope angles of anti-vortex blades and their arrangements were experimentally studied. The results showed that the discharge coefficient in the case with anti-vortex was more than the spillway without it. The efficiency of the morning glory spillways increased with the number of anti-vortex blades [5]. Enjilzadeh and Nohani [6] used Flow3D numerical models, boundary and inlet conditions, and grid spacing of flow field in different slope angles of anti-vortex blades and their arrangement modes. According to the results, the numerical model's relative error in determining the spillway discharge rate was 6.4%. The numerical model's relative error in calculating the flow depth parameter on the spillway crest was 6.7% compared to experimental results. The error of the numerical model in determining average flow velocity in the spillway crest equaled 7%, and the relative error for hydrostatic pressure of the flow on the spillway crest was 8.4%. Lashkar and Sheikhi [7] indicated that increasing the slope of inlet and outlet keys (Z) in Weirs as Crown Wheel spillways would increase the discharge flow rate, number of cycles at low heads, and flow discharge coefficient. Therefore, the discharge coefficient in a Crown Wheel spillway was 2.2 bigger than in a circular vertical sharp-edged weir. The circular piano key inlet increased overflow discharge capacity by about 15.16% compared to the shaft spillway. Also, the circular piano key inlets with an angle of 90 degrees had the best hydraulic performance [8]. The maximum error of calculating the discharge flow rate of the sectoral morning glory spillways equaled 7.77 % and occurred at a sector of 62 degrees using the three-dimensional numerical model [9]. Brakeni and Petrovic [10] concluded that the cross-section of the entrance with a 12-section polygonal configuration decreased the maximum water level during the full flood by 0.68 m. In addition, the new design increased the discharge coefficient up to 0.52, significantly reducing the risk of cavitation erosion of concrete. The flow discharges through marguerite-shaped inlets with holes at the bottom were approximately six, three, and two times greater than flow discharges through a simple shaft spillway, a circular piano key inlet, and a simple marguerite-shaped inlet, respectively. These inlets significantly reduced the water head over the waterways and increased the flow discharge due to the positive relationship between the flow discharge and crest length [11]. Chitsazan and Ghafouri [12] presented a computer simulation of effective anti-vortex blades (piers) methods. They showed that inserting two anti-vortex blades with a crest slope of 0° by a length of 8 meters between the spillway crest and throat decreased the water head and increased the spillway discharge coefficient to 0.53 and 5.58 times, respectively. The present study aims to decrease the upstream water depth of the dam with the same discharge by changing the shape of the inlet shaft spillway and the tailwater depth. Also, the study aims to compare the discharge coefficient between those cases to ward off the flood risk.

2.EXPERIMENTAL WORK

The experiments were conducted in the Hydraulics Laboratory at the University of Mosul in a 20m-long rectangular channel with glass walls 70 cm high and 80 cm wide. The shaft spillway was installed 3 m from the upstream channel, made from a transparent glass wall with a thickness of 0.4 cm, to ensure that no water leaked except through the spillway. Four models of shaft spillway inlets were used: The circular A1 model, a star shape with four prominences; B1 model, a star shape with eight prominences; and C1 model, a star shape with sixteen prominences E1 model, Fig.1. The protrusion height was 3 cm above the circular base of the spillway, with a thickness of 2 mm. The shaft spillway diameter was (15) cm, with a constant height of the shaft spillway edge to the bottom of the channel, i.e., 35cm. The horizontal distance from the transparent wall was 20 cm to the inner edge of the shaft overflow, Fig. 2. The perimeter and the area for each shape were calculated in Table 1. A barrel downstream of the outlet spillway was installed to control the tailwater level downstream. Therefore, three types of tailwater conditions were studied, i.e., free, submerged, and semi-flow (Fig. 3). The experiments started with a circular shaft spillway (A1) and free flow. The water depth level (H) reading at 50 cm upstream of the spillway entrance started from a 2cm water depth above the spillway edge and increased every 1 cm to guarantee ten water depths. Five low heads achieved an H/D ratio of less than 0.5, which was the case of the weir flow, while the others achieved an H/D ratio greater than 0.5, where the flow changed to the orifice flow. The discharge was pumped between (4.8 and 24.8) l/s. The tailwater was changed to semi-submerged at (18 cm). Then, all measurements were repeated. After that, the tailwater was changed to submerged at (28 cm). All these measurements with all previous cases were repeated with modified entrance shapes to cases (B1, C1, and E1), respectively. Hence, the total number of experiments was 120, i.e., 10 heights, 4 shapes, and 3 Tw.

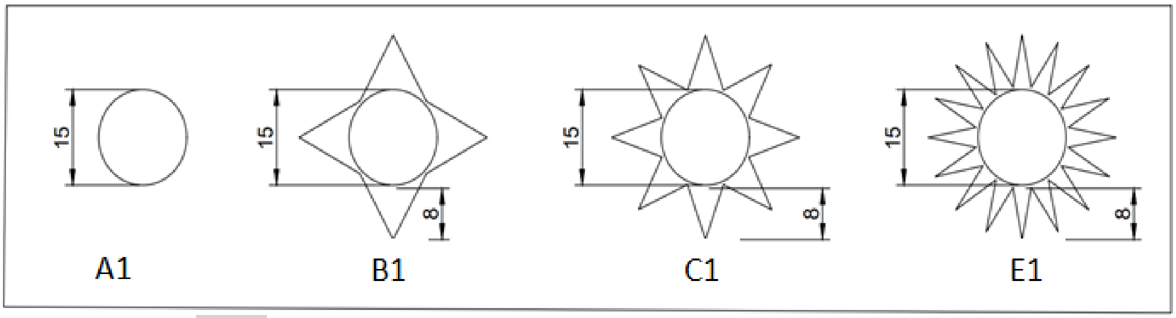

Fig. 1 The Cross-Section of the Vertical Overflow Entrance Shapes.

Table 1 The Area and Perimeter of the Shaft Spillway Entrance Shapes.

Shaft spillway diameter	Area and circumference	Shapes			
		A1	B1	C1	E1
(15 cm)	Area(cm²)	176.6	362.3	391.7	400.4
	Circumference(cm)	47.12	94.3	146.2	265.119

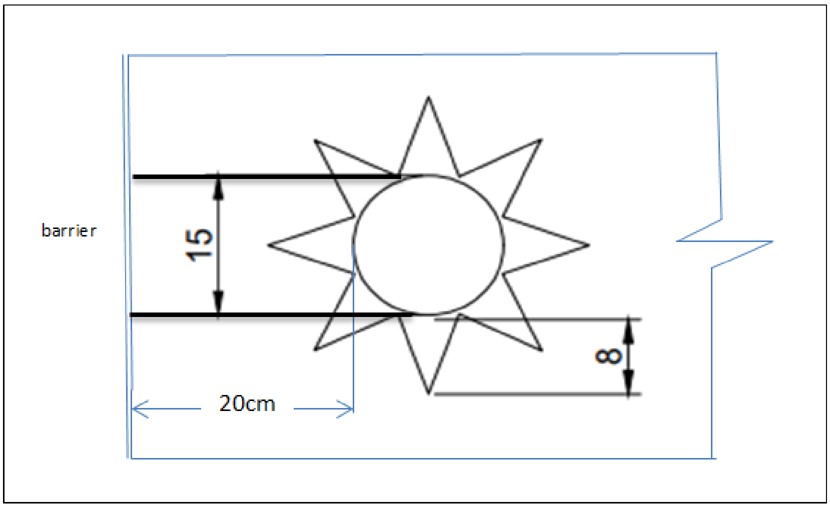

Fig. 2 Cross-Section of the Elbow Position.

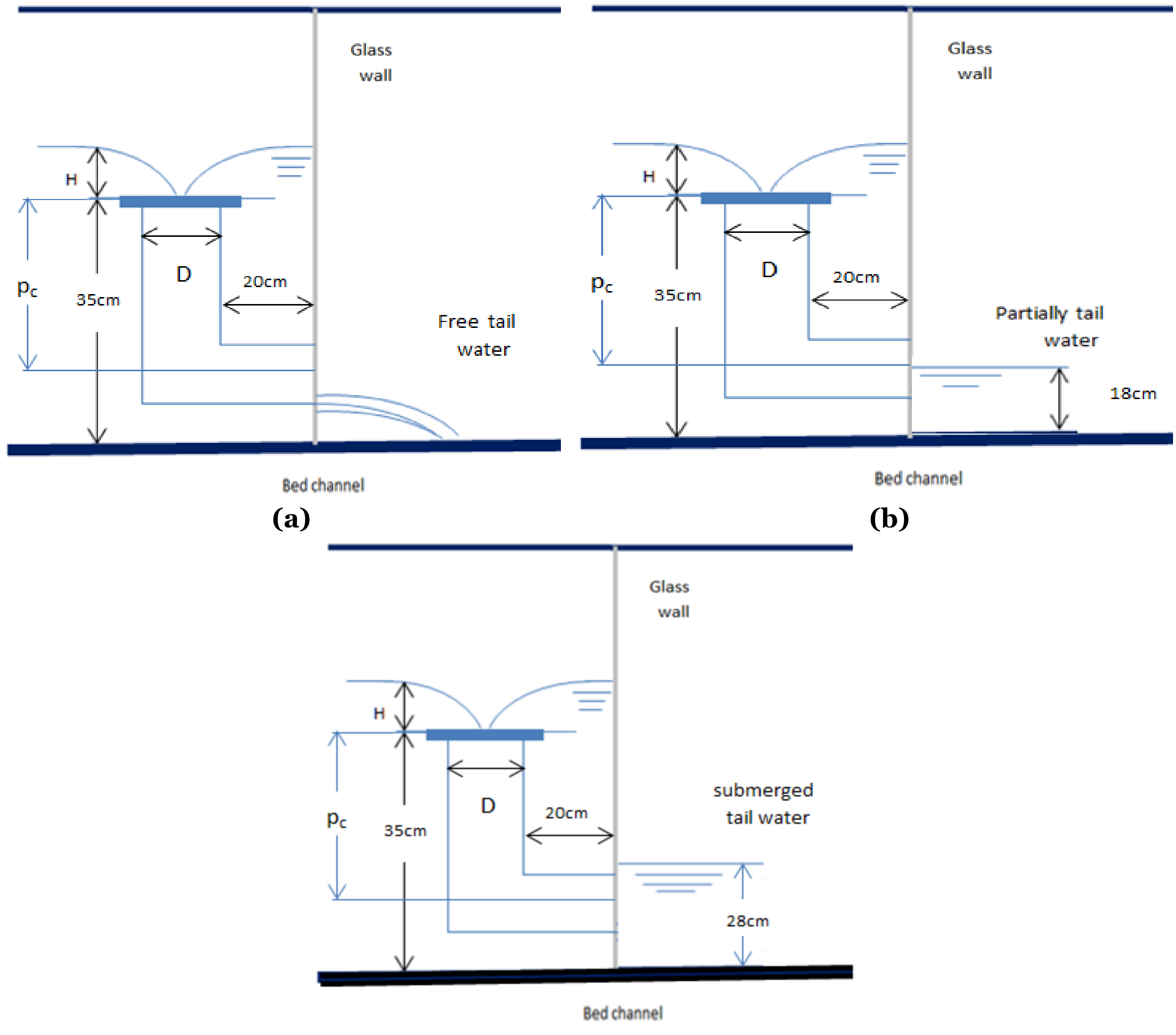

Fig. 3 Type of Tail Water Condition: (a) Free Tail Water Condition, (b) Semi-Tail Water Condition, and (c) Submerged Tail Water Condition.

3.THEORETICAL BACKGROUND

The actual discharge was calculated by sitting sharp rectangular crested weir at the end of the channel according to British standards [13- 15]:

$$Q = \left(0.4\left(h/p\right) + 3.22\right)(l - 0.003)(h + 0.003)^{3/2} \quad (1)$$

Where:
Q= actual discharge (ft3/s) (m^3/s) (l/s).
h= the head measured above the weir crest (ft)
l = the length of the weir crest (ft)
p= the height of the weir (ft)

According to the water depth upstream spillway edge entrance, there were two different flow regimes: weir flow when the H/D ratio was less than 0.5 and orifice flow when the H/D proportion was more significant than 0.5 [16, 17]. Recognizing this other kind of flow is necessary for theoretical calculation. The discharges for these cases were calculated for the diameter of the shaft spillway and for all the models studied in the experiments, as follows:

1- Calculating the Actual and Theoretical Discharge of the Weir from the Following Equations [16, 17]:

$$Q_{theoretical} = \frac{2}{3}\sqrt{2g}\, L\, H^{2/3} \quad (2)$$

$$Cd = Q_{act}/Q_{the} \quad (3)$$

Where
Q= discharge m^3/s
Cd= discharge coefficient(-)
H= water head over the shaft spillway crest(m)
g= ground acceleration(m/s^2)
L= the wetted circumference of the shaft spillway entrance(m), i.e., its length was considered according to the figures in Table 1.

2- Calculation of the Absolute Discharge and the Theoretical Discharge of the Orifice [16, 17]:

$$Q_{theoretical} = a\sqrt{2g(H + Pc)} \quad (4)$$

Where
a= cross-sectional area m^2 of the shaft spillway, according to the figures and Table 1. Pc= the distance between the center of the outflow hole and the upper edge of the spillway(m), and its value was 17cm for a 15cm Diameter.

In the case of submerged tail water, H is the difference between the water heights at the inlet H1 and outlet H2 of the vertical spillway since H=H1–H2 (cm).

4.DIMENSIONAL ANALYSIS

The dimensional analysis method was used to study the flow characteristics and relationship of the dimensionless parameters with the discharge coefficient in the flow regime of the weir and the orifice flow for all cases of the inlet shape and tail water condition previously mentioned. The factors affecting a discharge coefficient Cd at the vertical spillway that was adopted in this research were mass density ρ (M/L^3), surface tension σ (M/T^2), dynamic viscosity μ (M/L×T) of water, gravity acceleration g (L/T^2), channel width B (L), which is taken one channel width (constant), diameters of vertical spillway D (L) one diameter used (constant), the velocity of flow in the shaft spillway V (L/T), the height of water downstream (outlet) of shaft spillway Tw (L), water head over the weir crest H(L), and the crest length L (L). Expressed by Eq. (5).

$$c_d = f\,(\rho, \sigma, \mu, g, B, D, V, Tw, H, L) \qquad (5)$$

By adopting Buckingham's method (theorem-π) in dimensional analysis, the non-dimensional relationship reached is as follows:

$$c_d = f\left\{\frac{\rho V^2 D}{\sigma}, \frac{V^2}{Dg}, \frac{\rho V D}{\mu}, \frac{H}{D}, \frac{Tw}{H}, \frac{B}{H}, \frac{L}{H}\right\} \qquad (6)$$

Where ρ V^2 D/σ, V^2/D g, and ρ V D/μ are Weber (We), Froude (Fr), and Reynolds (Re) numbers, respectively. To prevent the viscosity and surface tension effects, Re was considered more than 10^4 [18, 19] and We more than 50 [20]. Therefore, Re and We were neglected, and the final result of the equation can be written as:

$$c_d = f\left\{Fr, \frac{H}{D}, \frac{Tw}{H}, \frac{B}{H}, \frac{L}{H}\right\} \qquad (7)$$

5.RESULTS AND DISCUSSION

This study experimentally investigated one diameter for a vertical shaft spillway and four entrance shapes, constant vertical and horizontal distances from the bottom and separation wall of the upstream channel, and three different tailwater cases downstream of the channel, i.e., free, semi, and submerged flow. Five water heights were considered for the channel upstream to achieve weir flow and five-depth verification orifice flow for all inlet shapes, as shown in Table 2, of the height values for the diameter of 15 cm.

5.1.Head-Discharge Condition Effect

The relationship between the actual discharge and the effective head (H) is shown in Fig. 4. It can be seen that the transitional area of the transformation of flow occurs between the depths (7.5 - 8.5) cm, which is the transitional point of the flow pattern from the weir to an orifice flow inside the shaft spillway. These heights are close to the radius of the shaft spillway in this experiment, i.e., 7.5 cm. The inlet shape switched to B1, C1, and E1, and the measurements were done for free flow conditions and then repeated for all cases (A1-E1) for semi and submerged states. All these cases are shown in Figs. 5-8.

Table 2 The Water Depth (H) Values Over the Shaft Spillway Crest for all Cases of Tailwater and Inlet Shapes. (All Dimensions in cm.)

A1(H)- Semi (cm)	A1(H)- Submerged (cm)	A1(H)- Free (cm)	Qact (l/s)
4.5	3.7	4.3	4.857
5.7	4.9	5.4	8.080
6.6	5.6	6.3	10.114
7.2	6.3	6.9	12.310
7.3	7.8	7.5	13.701
7.7	9.2	8.5	19.256
9.7	10.2	9.7	20.340
10	11.2	10.6	21.445
11.5	11.9	11.3	23.145
12.5	13.5	12.8	24.892
B1(H)- Semi (cm)	**B1(H)- Submerged (cm)**	**B1(H)- Free (cm)**	**Qact (l/s)**
3.4	3.1	3.3	4.857
4.3	3.8	4.1	8.080
4.9	4.3	4.6	10.114
5.7	4.9	5.2	12.310
7.4	7	7.3	13.701
7.5	8.5	8.3	19.256
8.7	9	8.6	20.340
9.4	10.5	9.8	21.445
10.6	11.4	10.7	23.145
12.3	12.9	12.4	24.892
C1(H)- Semi (cm)	**C1(H)- Submerged (cm)**	**C1(H)- Free (cm)**	**Qact (l/s)**
3.3	2.7	3.1	4.857
4.5	3.7	4	8.080
4.9	4.2	4.4	10.114
5.8	4.8	5.1	12.310
6.2	5.5	5.7	13.701
6.8	7.9	7.6	19.256
8.3	8.8	8.5	20.340
9.2	10.1	9.6	21.445
9.9	11	10	23.145
12	12.5	12.2	24.892
E1(H)- Semi (cm)	**E1(H)- Submerged (cm)**	**E1(H)- Free (cm)**	**Qact (l/s)**
2.5	2.1	2.2	4.857
3.3	2.8	3.1	8.080
3.8	3.2	3.5	10.114
4.5	3.7	4.1	12.310
5.2	4.3	4.6	13.701
6	5	5.5	19.256
8.2	8.7	8.3	20.340
8.9	9.9	9.4	21.445
9.8	10.6	9.65	23.145
11.5	11.8	11.7	24.892

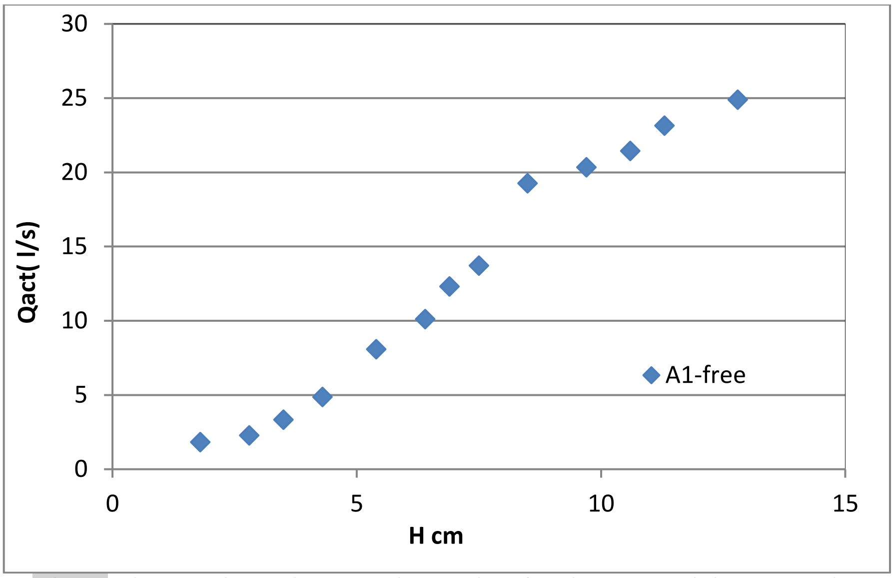

Fig. 4 The Head-Discharge Relationship for the A1-Model in Free Flow Condition.

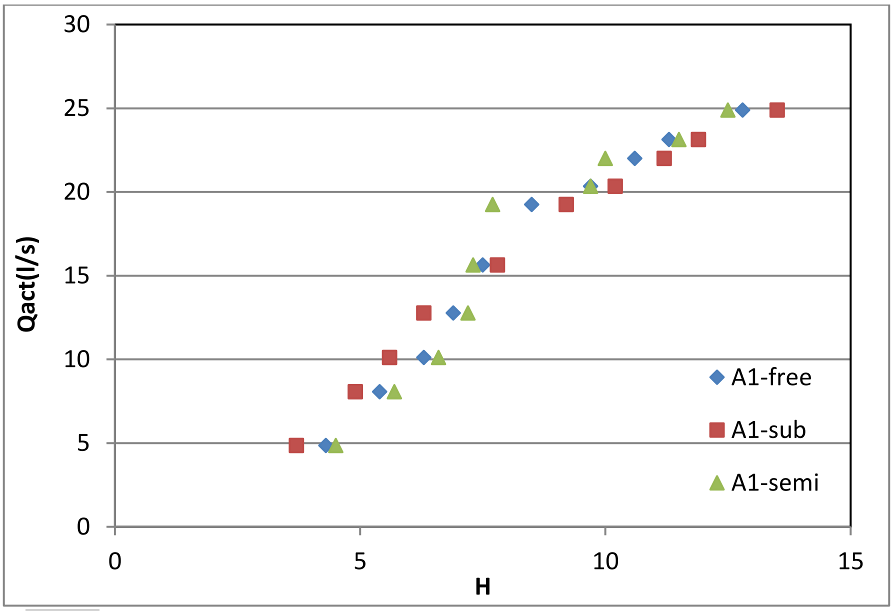

Fig. 5 The Head-Discharge Relationship in the A1-Model for Free, Semi, and Submerged Flow (for Tail Water Condition).

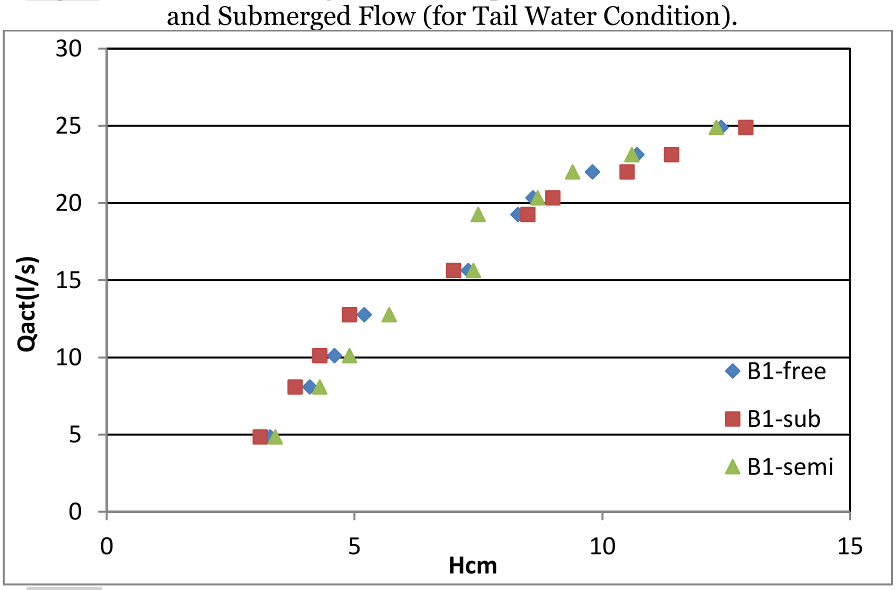

Fig. 6 The Head-Discharge Relationship in the B1 Model for Free, Semi, and Submerged Flow (for Tail Water Condition).

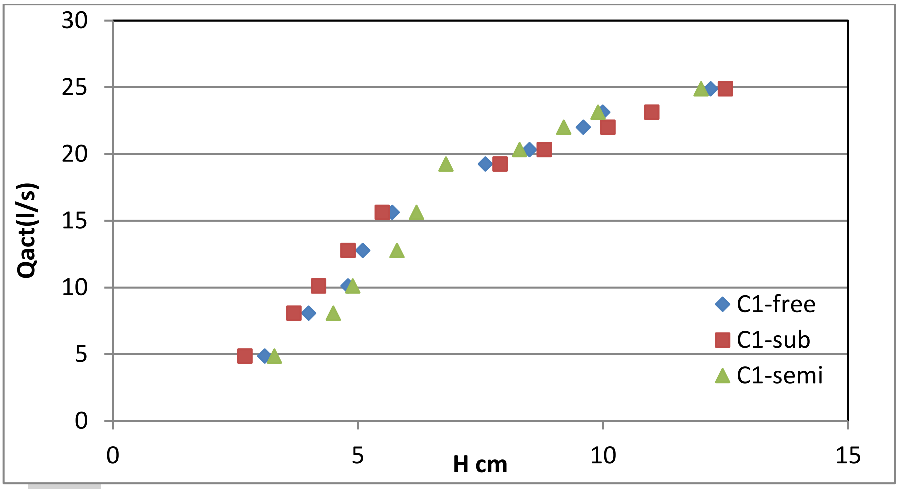

Fig. 7 The Head-Discharge Relationship in the C1-Model for Free, Semi, and Submerged Flow (for Tail Water Condition).

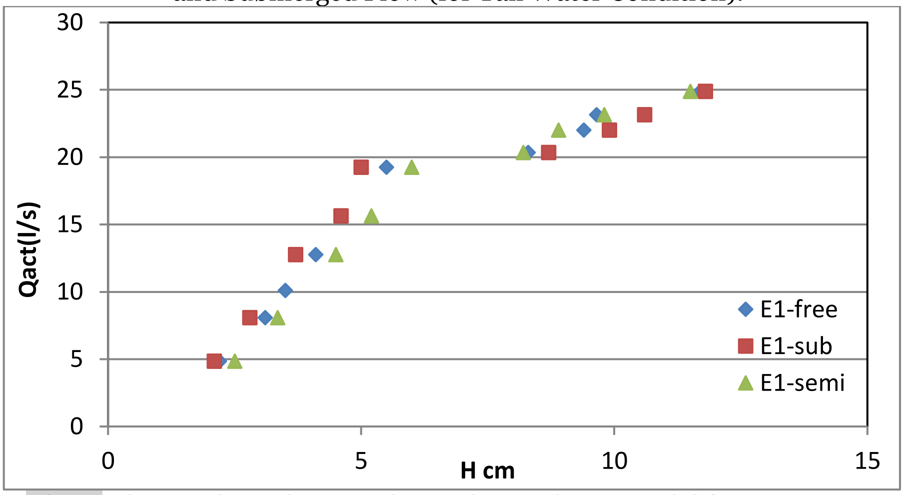

Fig. 8 The Head-Discharge Relationship in the E1 Model for Free, Semi, and Submerged Flow (for Tail Water Condition).

Figures 5 - 8 show the weir flow happens when the H/D values are under 0.5. In contrast, the orifice flow occurred when H/D values were above 0.5, with some differences according to entrance edge shape and tailwater conditions. In the case of the submerged weir flow regime, the water depth was 6% less than that of the free tailwater condition because the hydrostatic pressure at the outlet hole of the shaft spillway was less than the atmospheric pressure above the edge of the vertical spillway, increasing the water discharge outside the spillway and decreasing (H) [21, 22]. In contrast, at semi-submerged conditions, the water depth was 5% greater than the free flow. The free flow condition was an intermediate state between them. However, the shaft spillway entrance E shape resulted in the lowest height of the water surface of the overflow in the case of the submerged condition, i.e., 2.1 cm at the discharge 4.85 l/s. While these values increased to 2.7, 3.1, and 3.7 cm for models C1, B1, and A1, respectively, at the same discharge. In the case of the orifice flow regime, the semi-submerged condition resulted in a minimum value of H, while the submerged state resulted in maximum values. Their depths were greater than those of free flow condition by 3% because the fluid pressure at the submerged case outlet was more significant than the inlet. This additional pressure from water depth reduced the discharge from the spillway; thus, H increased [22, 19]. Figure 9 shows that the water depth gradually decreased when changing the inlet shapes from A1 to E1 because the perimeter of the crest edge increased flow discharge and decreased head-on crest. When the flow type was similar to the flow over the weir, the length of the upper edge of that weir effectively increased its performance. While in orifice flow and submerged, the wider inlet caused less—energy loss. Therefore, the minimum height of water depth happened at the E-shape for all tailwater conditions. Therefore, in the weir and office flow regime, the effect of changing the inlet shape was similar. The results indicated a decrease in water depth to 40% for the E1 model compared with A1 in the weir flow condition and 13% in the orifice flow condition, which is more significant for increased discharge. This pattern appeared in all tailwater conditions.

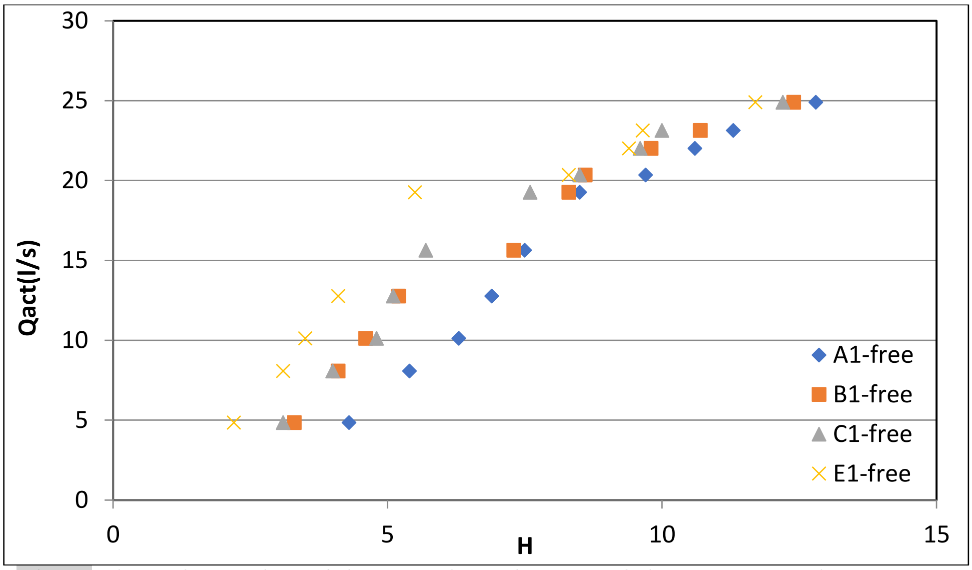

Fig. 9 The Relationship of the Actual Discharge and the Water Depth Upstream Spillway with the Effect of Four Inlet Shapes and Free Flow Condition.

5.2.Coefficient of Discharge Condition Effect

Figure 10 compares the Cd values of weir flow versus dimensionless parameters H/D. It illustrates the effect of inlet shape for models A1, B1, C1, and E1 in free, semi, and submerged tailwater conditions. In general, it can be seen that the discharge coefficient increased with the parameter H/D for four inlet shapes [23, 24]. In a free state, the maximum values of Cd at circular inlet shape A1 ranged from 0.39 to 0.5 and decreased gradually at B1, C1, and E1 inlet shape. The Cd values converted at the minimum range (0.16-0.196) for the same discharge flow, achieving a percentage of 58.8% for the A1 model higher than E1 (for all tailwater conditions). On the other hand, the Cd ranged in the case of free, submerged, and semi-submerged states were (0.16-0.506), (0.2-0.581), and (0.16-0.48), respectively, with the exact behavior of the crest shape effect. The lower values of Cd obtained at the semi-state were less than those obtained at the free state by 9.3%, while the submerged state resulted in the highest Cd, i.e., 17.76% more than the free state for weir flow, because the submerged state resulted in a lower value of H. Figure 11 shows the relation between Fr and Cd. The Cd values increased with Fr, and these increases were greater in the A1 and B1 models than in C1 and E1. These values were between (0.27-0.58) and (0.16-0.28) for all tailwater conditions. Figure 12 depicts the relation between Cd and L/H. The significant increase in L/H for all tailwater conditions decreased Cd, with maximum Cd values at model A1. Because of the large crest length of models B1, C1, and E1 compared to A1, the ratio L/H increased by reducing the head value (H) according to the different lengths of crest models. However, the tailwater condition effect follows the same trend as the last phenomenon, demonstrating that a submerged state obtained the largest Cd values. Figure 13 shows the relationship between Cd and the dimensionless factor Tw/H for four crest models and three tailwater states. Figure 13 shows that when Tw/H decreased, Cd values increased. The E1 model resulted in maximum Cd values, i.e., 3.5% higher than the A1 in free and semi-submerged states. It is clear that the average values of Cd in submerged Tw were higher than those in free and semi-Tw. The A1 model's Cd for the submerged state decreased by a small percentage compared to other models. The average Cd values in free and semi-submerged conditions were higher than those in submerged conditions. In other words, the Cd values increased by increasing H/D in the same trend of weir flow for all crest shapes and tailwater conditions, as shown in Fig. 14. Figure 15 shows that the Cd values increased with Fr in the weir flow condition. In contrast, the Fr values in the orifice flow condition were closer to each other for all tailwater states because Fr depends on the diameter of the shaft spillway in the orifice flow, which was constant at 15 cm. Therefore, it can be deduced that the Cd values in free and semi-submerged conditions were closer, while in the submerged state, they were more than the latter. Figures 16 and 17 show that increased L/H and Tw/H reduced the Cd values. The highest Cd values at the E1 model for full-submerged state correspond with H/D and Fr vs Cd in Figs. 14 and 15. Finally, the Cd values were very convergent in the orifice flow regime. As a result, the spillway entrance shape E was the best model to reduce the risk of flood due to increasing the perimeters and discharge coefficient, and the water surface of the dam advance was less than the other shapes and for the same discharge.

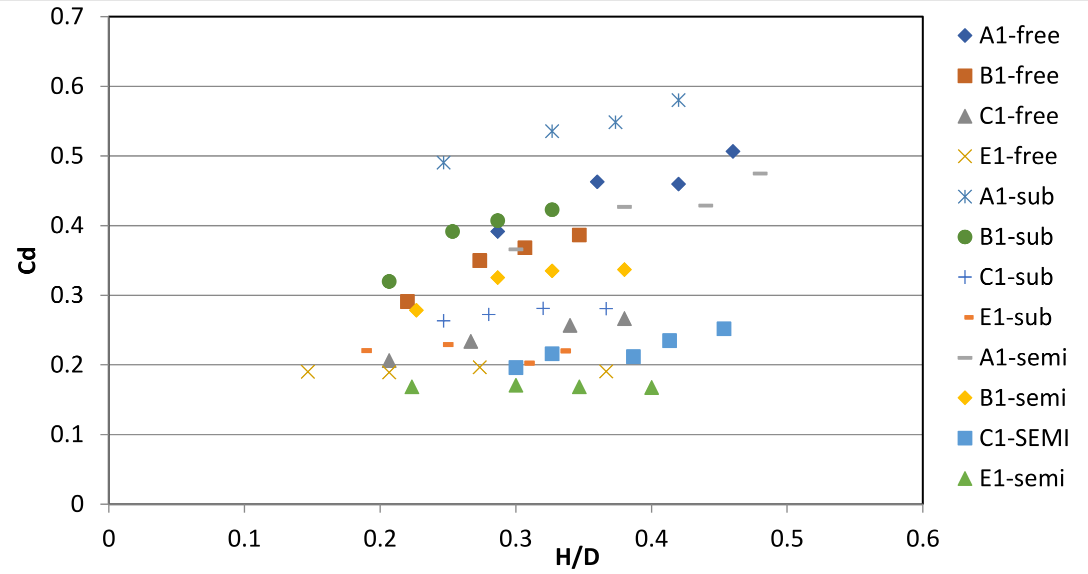

Fig. 10 The Relationship of Cd with the Parameter H/D for All Models and Three Conditions of the Tailwater in the Weir Flow Regime.

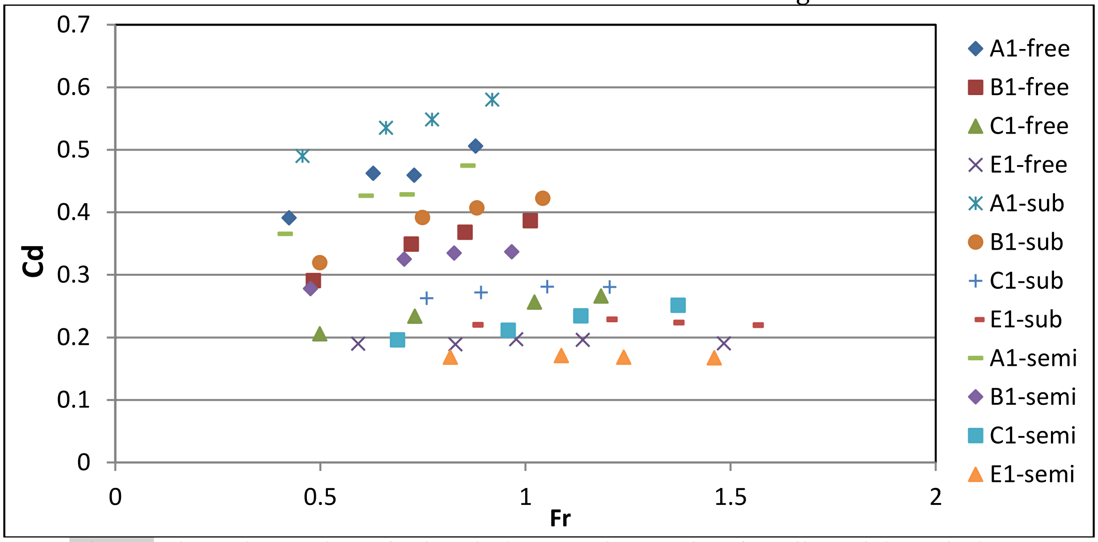

Fig. 11 The Relationship of Cd with the Froude Number for All Models and Three Conditions of the Tailwater in the Weir Flow Regime.

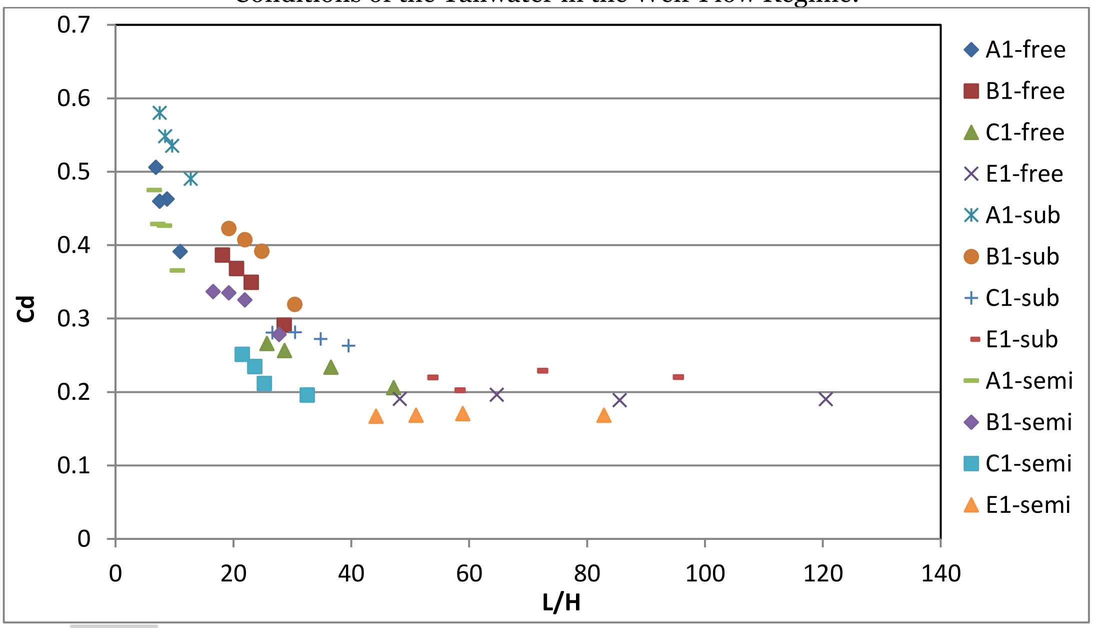

Fig. 12 The Relationship of Cd with the Parameter L/H for All Models and Three Conditions of the Tailwater in the Weir Flow Regime.

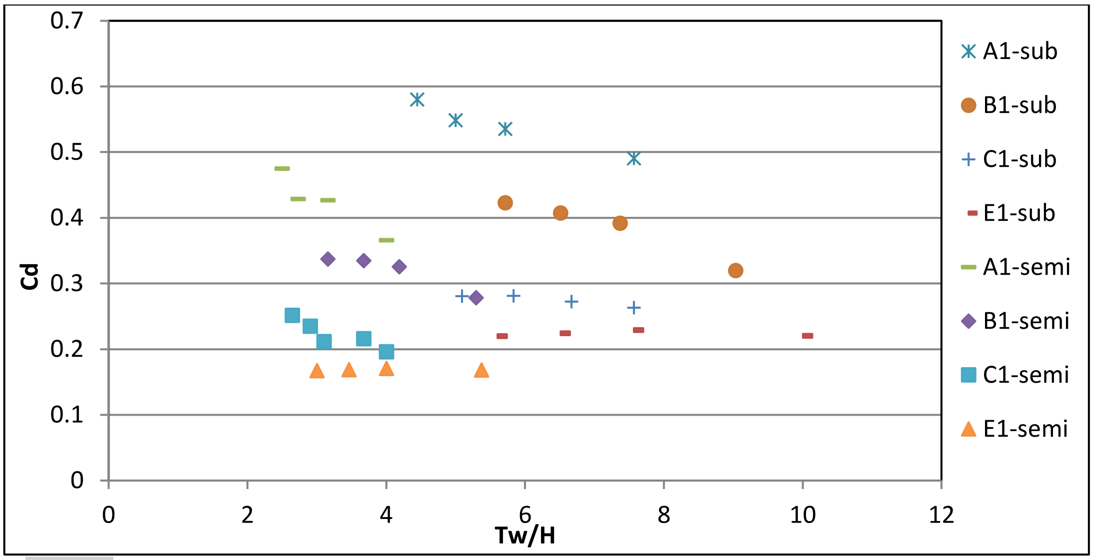

Fig. 13 The Relationship of Cd with the Parameter Tw/H for All Models at Sub and Semi-Sub Conditions of the Tailwater in the Weir Flow Regime.

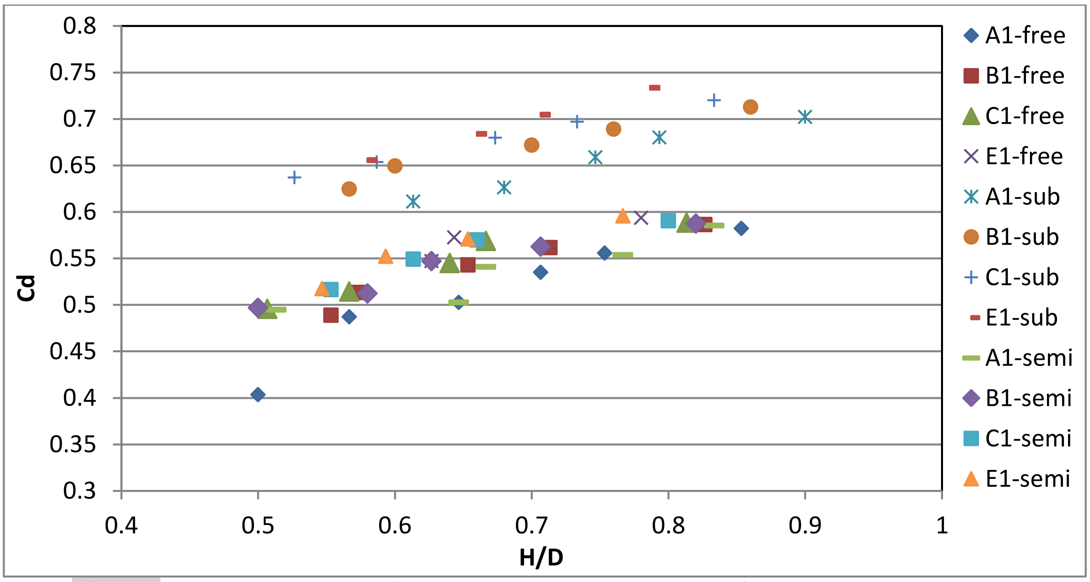

Fig. 14 The Relationship of Cd with the Parameter H/D for All Models and Three Conditions of the Tailwater in the Orifice Flow Regime.

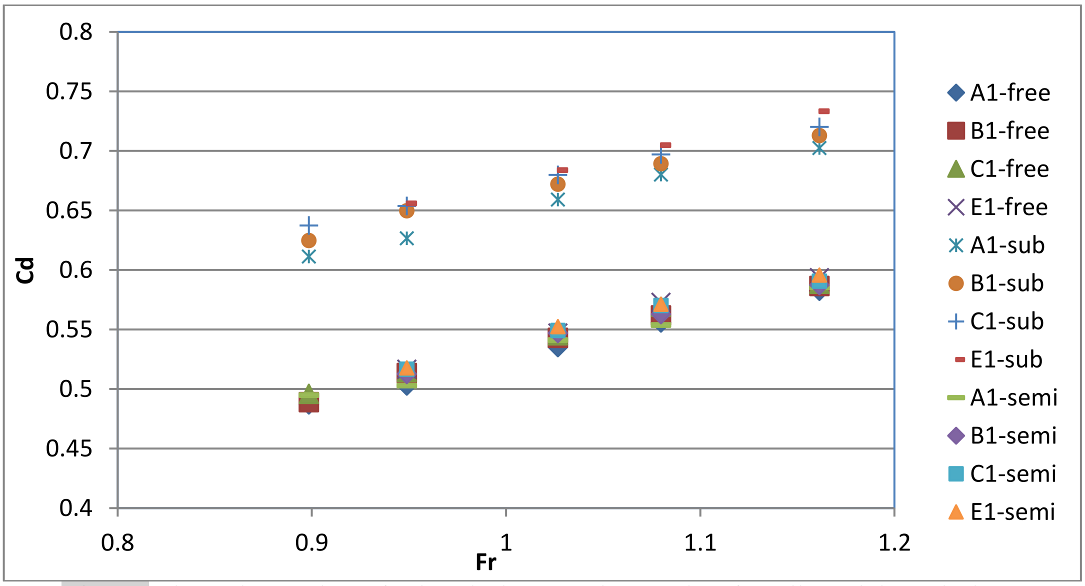

Fig. 15 The Relationship of Cd with the Froude Number for All Models and Three Conditions of the Tailwater in the Orifice Flow Regime.

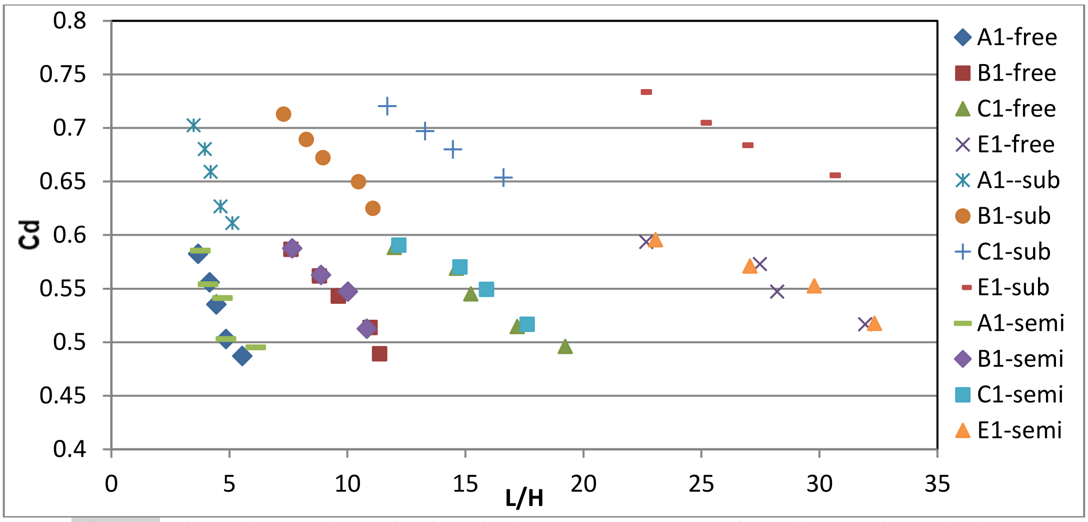

Fig. 16 The Relationship of Cd with the Parameter L/H for All Models and Three Conditions of the Tailwater in the Orifice Flow Regime.

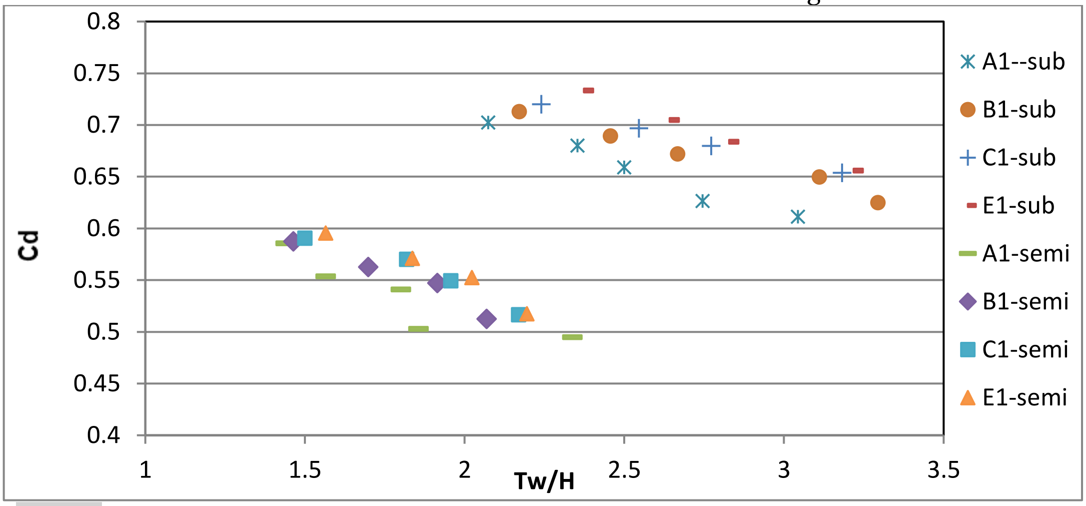

Fig. 17 The Relationship of Cd with the Parameter Tw/H for All Models at Sub and Semi-Sub Conditions of the Tailwater in the Orifice Flow Regime.

6.CONCLUSIONS AND RECOMMENDATIONS

1) Two flow conditions for water depth were above the spillway: weir flow when H/D values were less than 0.5, and orifice flow when H/D values were more significant than 0.5.

2) Water depth H decreased when the entrance crest length increased, increasing discharge flow.

3) The discharge coefficient values decreased with crest length. For all crest shapes, the maximum values in the weir flow condition occurred at submerged conditions.

4) In the weir flow regime, the discharge coefficient increased with H/D and Fr. At the same time, these values decreased when L/H and Tw/H increased, with the most significant values at the A1 model in all tailwater conditions.

5) It is important to study the scour depth downstream vertical shaft spillway under changing other conditions rather than the above conditions.

ACKNOWLEDGMENTS

The authors sincerely thank the anonymous reviewers for their valuable suggestions in improving the manuscript.

NOMENCLATURE

a	cross-sectional area of the m2 columnar extruder inlet shape of the columnar extruder.
Cd	discharge coefficient.
D	diameter of the vertical overhang in cm.
G	ground acceleration m/s.
H	the height of the water at a distance of 50 cm from the front of the vertical face, m.
L	wetted circumference of the shaft spillway inlet m.
Pc	the distance from the edge of the CREST vertical extrusion to the center of the horizontal part of the vertical extrusion, m.
Q	discharge m3/s.

REFERENCES

[1] Nohani E. **An Experimental Study on the Effect of Vortex Breakers on Discharge Coefficient for the Shaft Spillways With Sharp Edge and Wide Edge**. *Journal of Civil Engineering Urban* 2014; **4**(5): 546–549.

[2] Khaleel FI, Mohammed AY. **The Effect of Dual Water Jet on Discharge**

Coefficient of Vertical Spillway. *Al-Rafidain Engineering Journal* 2021; **26**(2): 292–299.

[3] Bagheri A, Bajestan MS, Jahromi HM, Kashkooli H, Sedghee H. **Hydraulic Evaluation of the Flow Over Polyhedral Morning Glory Spillways**. *World Applied Science Journal* 2010; **9**(7): 712–717.

[4] Nohani E, Naghshine H. **Experimental Evaluation of the Anti-Vortex Plates Angle on Discharge Coefficient for the Shaft Spillway**. *International Journal of Agriculture* 2013; **3**(2): 246.

[5] Hajipour G. **Experimental Investigation of the Effect of Angular Vortex Blades on Discharge Angular Vortex Blades Against Nilofri Overflow Discharge**. MSc Thesis. School of Water Sciences, Shahid Chamran University of Ahvaz, 2014.

[6] Enjilzadeh MR, Nohani E. **Numerical Modeling of Flow Field in Morning Glory Spillways and Determining Rating Curve at Different Flow Rates**. *Civil Engineering Journal* 2016; **2**(9): 448–457.

[7] Lashkar B, Sheikhi Y. **Introduce of Crown Wheel Spillway and Study of its Discharge Coefficient under Free Flow Regime**. *Journal of Irrigation Science Engineering* 2017; **40**(2):209–221.

[8] Kashkaki Z, Banejad H, Heydari M, Olyaie E. **Experimental Study of Hydraulic Flow of Circular Piano-Key Inlet in Shaft Spillways**. *Journal Rehabil Civil Engineering* 2019; **7**(3): 96–102.

[9] Sabeti P, Karami, H, Sarkardeh H. **Analysis of the Impact of Effective Length of Morning Glory Spillway on its Performance (Numerical Study)**. *Instrumentation Mesure Metrologie* 2019; **18**(2): 211–221.

[10] Brakeni A, Petrovic GA. **An Experimental Study of Shaft Spillway with a Polygonal Section**. *UPB Scientific Bulletin, Series D: Mechanical Engineering* 2020; **82**(2): 255–268.

[11] Maedeh K, Kabiri SA. **Effects of Modern Marguerite-Shaped Inlets on Hydraulic Characteristics of Swirling Flow in Shaft Spillways**. *Water Science Engineering* 2021; **14**(3): 246–256.

[12] Chitsazan M, Ghafouri HR. **Optimization of Anti-Vortex Blades Geometry in Morning Glory Spillways by Numerical simulation**. *SSRN Electronic Journal* 2022; **5**(1): 1-27

[13] Bengtson HH. **Sharp-Crested Weirs for Open Channel Flow Measurement**. *Continuing Education and Development* 2011; **2**(C02-022): 1-25.

[14] Irzooki RH, Najem AS. **Study the Affecting Factors on Free Overfall Flow and Bed Roughness in Semi-Circular Channels by Artificial Neural Network Neural Network**. *Tikrit Journal of Engineering Sciences* 2022; **29**(4): 69–78.

[15] Luqman LS, Kawa ZA. **Advancements in Flow Behavior Investigation and Performance Enhancement of Morning Glory Spillways: a Systematic Review of Numerical and Physical Models**. *Iranian Journal of Science and Technology- Transactions of Civil Engineering* 2023; **47**(5):1–35.

[16] Jalil SA, Hussein BS, Sarhan SA. **Visualization of Elbow Flow Performance as Shaft Spillway**. *Ain Shams Engineering Journal* 2020; **11** (4): 865–873.

[17] Gupta RS. **Hydrology and Hydraulic Systems**. Waveland Press, Inc; 2016.

[18] Anwar HO, Weller JA, Amphlett MB. **Similarity of Free-Vortex at Horizontal Intake**. *Journal of Hydraulic Research* 1978; **16**(2): 95–105.

[19] Karim RA, Mohammad JR. **SPH Open Boundary Simulation of Free-Surface Flow Over Ogee-Crested Spillway**. *Tikrit Journal of Engineering Sciences* 2021; **28**(2): 137–151.

[20] Machiels O, Pirotton M, Pierre A, Dewals B Erpicum S. **Experimental Parametric Study and Design of Piano Key Weirs**. *Journal of Hydraulic Research* 2015; **53**(4): 543–545.

[21] Mussalli YG. **A Study of Flow Conditions in Shaft Spillways.** Institute of technology. Ph.d Thesis In the School of Civil Engineering: 1970.

[22] Zayed M. **Lecture Notes (Flow Through Orifices)**. 2020; 1-12.

[23] Christodoulou G, Mavrommatis A, Papathanassiadis T. Experimental Study on the Effect of Piers and Boundary Proximity on the Discharge Capacity of a Morning Glory Spillway, Proceedings of the 1st IAHR Europe Congress (Edinburgh, 2010).

[24] Aydin MC, Ulu AE **Numerical Investigation of Labyrinth-Shaft Spillway**. *Applied Water Science* 2023; **13**(4): 89-99.